EPRI Analysis for Determining the 95/95 Confidence Limits on CASMO-5 Hot Full Power (HFP) Measured Reactivity Decrement Bias Regressions Used in the EPRI/Studsvik Burnup Benchmark

This attachment provides a step-by-step summary of the individual pieces of the analysis (agreed to in recent NRC/EPRI/NEI discussions) that have been implemented to produce **95/95 confidence limits** for the measured Hot Full Power (HFP) PWR fuel reactivity depletion decrement biases derived from Duke reactor data as documented in EPRI Technical Report 1022909 [1].

Summary of Analysis Procedure

The steps in the overall procedure to compute statistical confidence limits for the reactivity decrement bias curves derived using the EPRI methodology and measured data are as follows:

1. Using all the >2500 HFP sub-batch points in the original EPRI report, generate a master database containing: a unique sub-batch/cycle index, the sub-batch burnup, the sub-batch sensitivity, and the sub-batch reactivity decrement bias.

2. Plot the reactivity decrement bias vs. sub-batch sensitivity and perform a quadratic regression to determine the 95% prediction interval for the reactivity decrement bias versus sub-batch sensitivity.

3. Approximate the individual sub-batch reactivity decrement bias variances from the spread of the 95% prediction interval curves (of the reactivity decrement bias regression vs. sub-batch sensitivity) by using the individual sub-batch sensitivities.

4. Determine the uncertainty of individual reactivity decrement bias data points from a quadratic function of sub-batch burnup, and combine this uncertainty with the sub-batch sensitivity variance to get a total variance estimate for each of the >2500 data points.

5. Collect all the >2500 HFP reactivity decrement bias data, and collapse all data within an individual sub-batch/cycle to one average value of reactivity decrement bias by statistically combining with the appropriate individual data variances. (This is the assumption of 100% correlation within a sub-batch/cycle.)

6. Perform a Weighted Least Squares (WLS) nonlinear regression fit to the collapsed reactivity decrement bias data versus sub-batch burnup, and compute the 95% confidence intervals for the regression fit.

7. Perform a Shapiro-Wilk test to determine if the data “passes the normality test,” so that confidence limits can be correctly interpreted.

8. Perform Step A, Step B, and Step C as outlined below to determine the CASMO-5 bias and its 95/95 confidence limits.

Step 8 of this procedure for assigning 95/95 confidence limits to the CASMO-5 reactivity decrement regression curves requires expansion and clarification because **we are not interested in a 95/95 confidence limit on the next measured data point – but rather we seek a 95/95 confidence limit on an underlying population parameter** (e.g., the regression model bias). We want to be 95% confident that the assigned uncertainty limits have a 95% likelihood of bracketing the true (and unknown) bias.

This three-step procedure is:

Step A) Split the EPRI measured data into two enrichment ranges (a lower half and an upper half) and perform regression analysis of the data separately for both halves, and construct two independent regression curves. If the regression curve of the bias vs. burnup were independent of the sub-batch, the two curves would be identical (in the limit of infinite number of sub-batch measurements).

Step B) Construct the curve of absolute difference in biases between the two enrichments ranges and add (subtract) this curve to upper (lower) regression 95% confidence interval of the full data regression – to obtain an augmented estimate of the confidence interval of reactivity decrement bias. By doing this, we are making the implicit (and conservative) assumption that the full absolute difference in biases between the two enrichment ranges is applicable to the bias uncertainty for all fuel enrichment sub-batches.

Step C) Multiply the augmented 95% confidence intervals by the ratio of the two-sided tolerance limit actor for (95%, 95%, # sub-batch/cycles) to the Student's t-value for (95%, # of sub-batch/cycles) to estimate the 95% confidence limit. This step is necessary since we seek a 95/95 confidence limit on the regression fit to reactivity decrement bias. Note that the Student's t-value is used in constructing regression confidence intervals, and here we are making the additional assumption that the underlying **distribution of residuals is Gaussian**.

In subsequent NRC/EPRI/NEI discussions (ML15351A117), it was also agreed to add an additional step to the analysis procedure between (steps 4 and 5) to correct for assumption that reactivity decrements have been computed from batch-averaged burnups, and there is an additional component of bias and uncertainty that accounts for **intra-batch burnup distribution effects**.

<u>Implementation of the Analysis Procedure</u>

Step 1 was implemented to generate a new master database that contains: a unique sub-batch/cycle index, the sub-batch burnup, the sub-batch sensitivity, and the sub-batch reactivity decrement bias. This database contains 2856 reactivity decrement biases as derived from the summary files of the 3 million CASMO-5/SIMULATE-3 cases that were run for the original EPRI/Studsvik report. Figure 1 displays the unfiltered individual data points for high and low enrichment sub-batches and also the 5% reactivity decrement (e.g., Kopp) bounds at HFP.

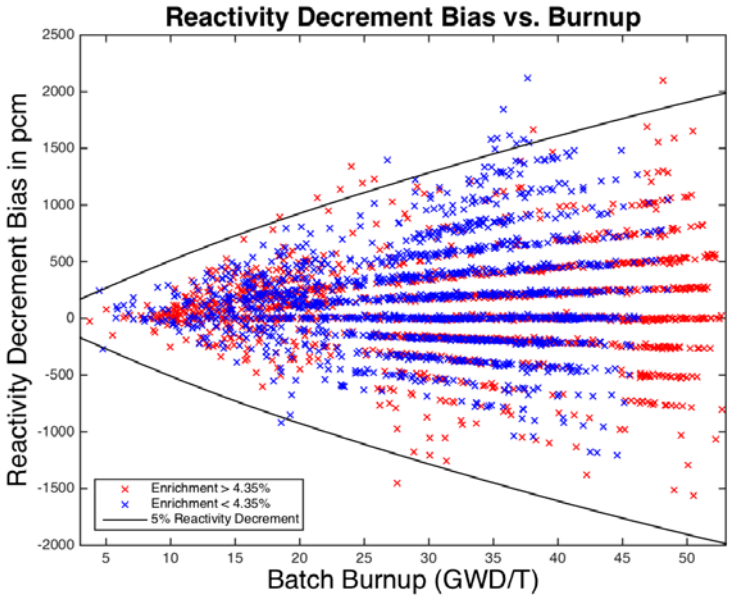

Figure 1 Measured Casmo-5 Reactivity Decrement Biases vs. Sub-batch Burnup

For Steps 2-3 of the analysis, reactivity decrement bias data was plotted vs. sub-batch sensitivity, and a quadratic regression was performed to determine the 95% prediction interval for the reactivity decrement bias versus sub-batch sensitivity, as displayed in Figure 2.

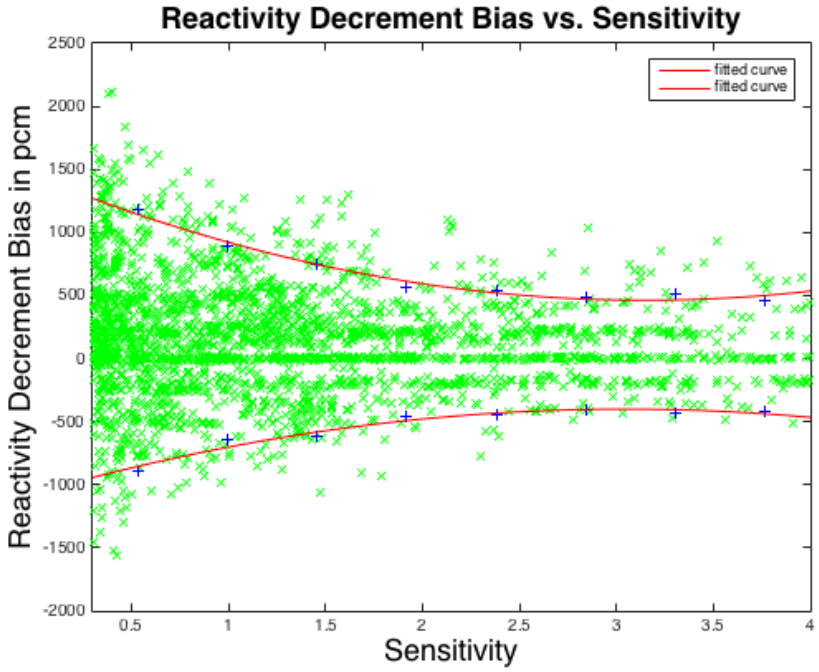

Figure 2 Reactivity Decrement Bias vs. Sub-batch Sensitivity

The 95% confidence interval was used to compute the normalized shape of 2-sigma variation versus sensitivity and the square of this variation (the variance) was fit to a quadratic polynomial and normalized as displayed in Figure 3. The data was fitted only up to a sensitivity of 4.0%, as the data

becomes exceedingly sparse at the higher sensitivity end of the data. The plus signs in this figure are variance points as determined using the Matlab VAR function for eight separate sub-batch sensitivity bins - just to make sure the fit was reasonable.

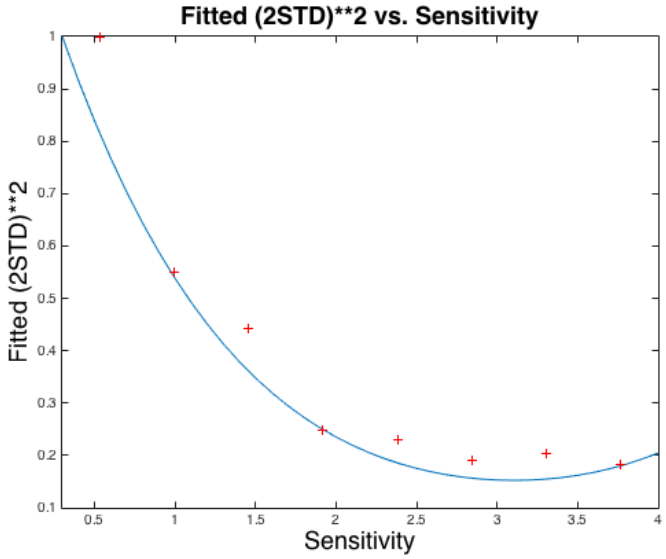

Figure 3 Reactivity Decrement Quadratic Fit vs. Sub-batch Sensitivity

For Step 4 of the analysis, reactivity decrement bias data (with a sensitivity screening parameter of 0.9%) was plotted vs. sub-batch burnup and a quadratic regression was performed to determine the 95% prediction interval for the reactivity decrement bias versus sub-batch burnup, as displayed in Figure 4.

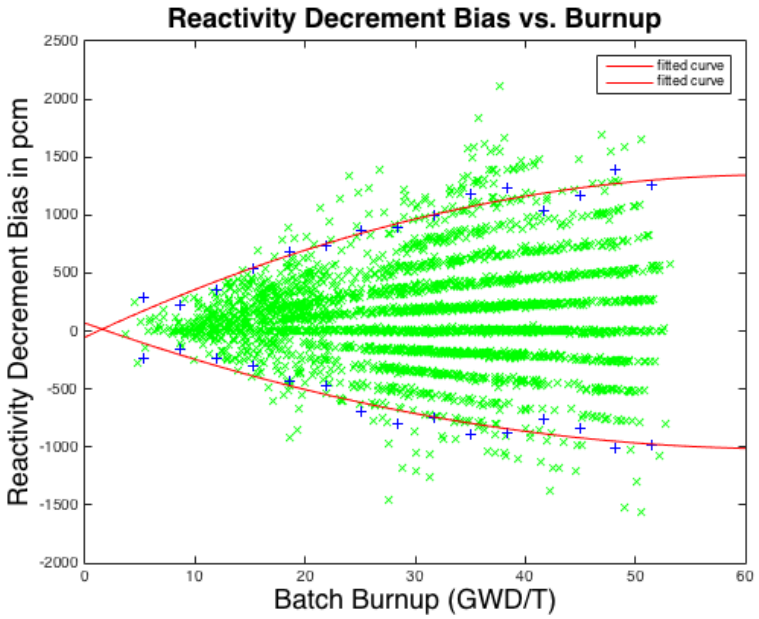

Figure 4 Reactivity Decrement Bias vs. Sub-batch Burnup

The fitted 95% confidence interval was used to compute the shape of 2-sigma variation versus burnup, and the square of this variation (the variance) was fit to a quadratic polynomial and renormalized as displayed in Figure 5. This figure also contains variance points as determined using the Matlab VAR function for fifteen separate sub-batch burnup bins - just to make sure the fit was reasonable.

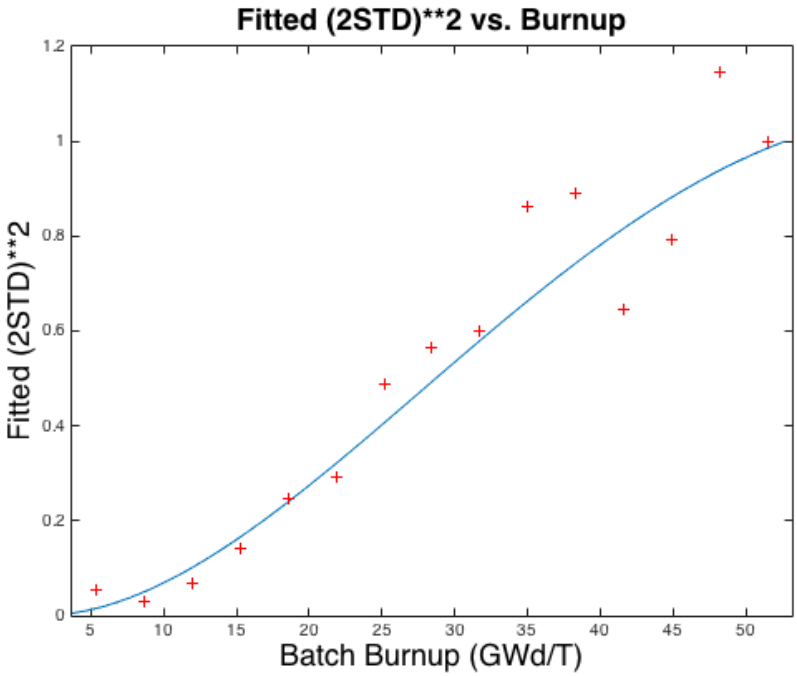

Figure 5 Reactivity Decrement Quadratic Fit vs. Sub-batch Burnup

The fitted variances curves were renormalized to a maximum 1.0, and total variance weights were computed as the sum of the reciprocal of the two fitted variances evaluated at individual sub-batch sensitivity and sub-batch burnup for each of the 2856 data points. These weights were used in the subsequent regression analysis using Weighted Least Squares (WLS), and Figure 6 displays the regression fit with the sensitivity screening parameter value of 0.9% (used for all the subsequent analysis in this note; to match that used in the original EPRI/Studsvik report [1]). **Note that the plotted prediction intervals correspond to the unfiltered data of all 2856 points.** Figure 7 displays a corresponding regression fit using un-weighted Ordinary Least Square (OLS) regression of the 1813 fitted data points.

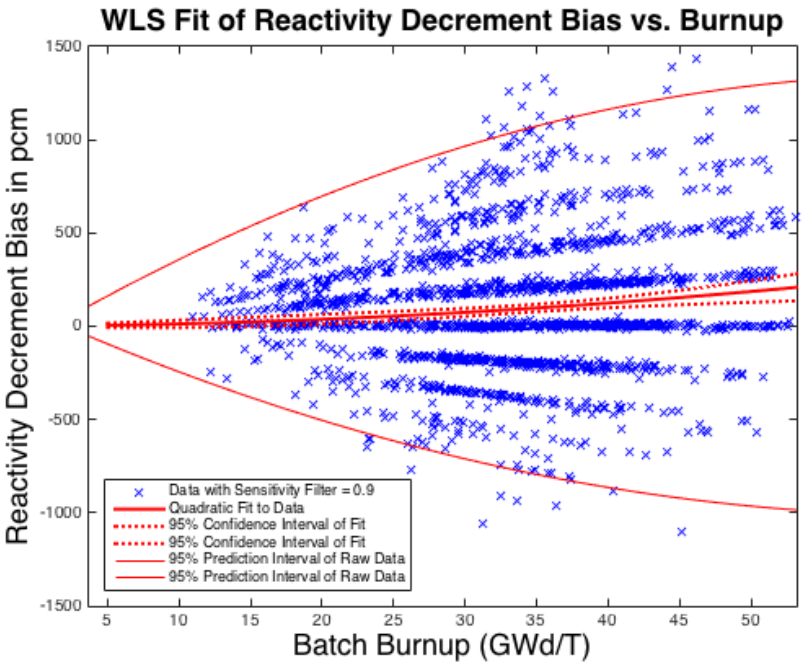

Figure 6 Reactivity Decrement Quadratic WLS Regression vs. Sub-batch Burnup

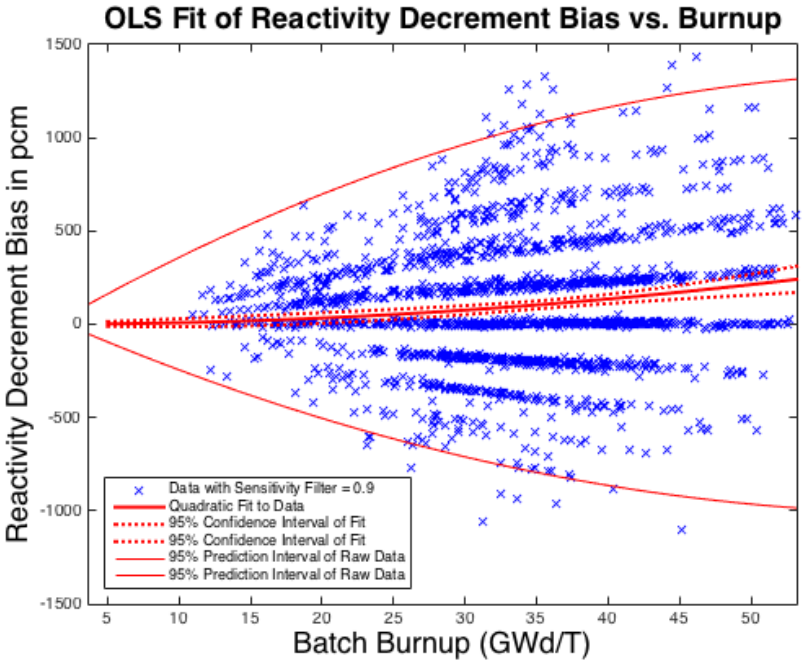

Figure 7 Reactivity Decrement Quadratic OLS Regression vs. Sub-batch Burnup

Despite large weight function changes with sub-batch burnup and sensitivity, both regressions produce very similar fits. The fact that the weights have little impact on the regression fits implies that measured

reactivity decrement biases are not sensitive to estimates of the dependence of variance on sub-batch burnup and sensitivity.

The additional step between Steps 4 and 5 (to correct for assumption that reactivity decrements have been computed from batch average burnups) was implemented by evaluating the maximum value of the second derivative of reactivity within each sub-batch/cycle burnup range, and multiplying this second derivative by the **maximum difference of assembly burnup from the sub-batch average burnup**. These reactivity decrement additions are displayed in the Figure 8.

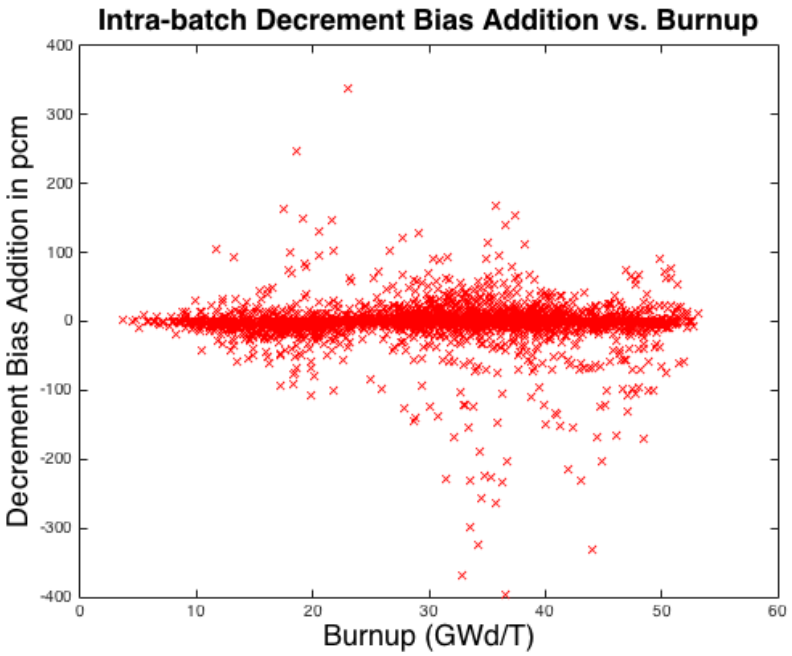

Figure 8 Intra-batch Reactivity Decrement Bias Addition vs. Sub-batch Burnup

The magnitude of this correction is very small for most data points because either the slope of reactivity is very constant within the range of batch burnup within a cycle, or because the range of intra-batch burnup itself is very small. When averaged over all data points, the average intra-batch burnup range is 1.97 GWd/T in absolute units and 10.6% in relative terms – not very large. Note that the implementation of this correction was performed with three conservative assumptions: 1) the change in derivative of reactivity was evaluated at its maximum point anywhere within the sub-batch/cycle, 2) the intra-batch burnup range of each sub-batch data point was taken to be the maximum value – even if it corresponded to only a single assembly in the sub-batch, and 3) the sign of the addition to each decrement bias was selected to maximize the absolute value of reactivity decrement bias. The impact of the intra-batch burnup variation addition is almost negligible, as it produced a maximum change in reactivity decrement bias regression fit of only 12 pcm.

Step 5 was implemented by collapsing all data within individual sub-batch/cycles to one average value of reactivity decrement bias per cycle by statistically combining individual reactivity decrement biases and their respective weights (i.e., reciprocal variances.) This is the assumption of 100% correlation of data within a sub-batch/cycle that is necessary so regression fit confidence intervals can be applied correctly (given that we cannot know the precise intra-cycle correlation of data that would be needed to use

individual data points). When collapsed over each cycle, there are 191 sub-batch/cycle reactivity decrement bias points for the subsequent analysis.

For Step 6, these collapsed data values were used in a Weighted Least Squares (WLS) quadratic regression fit as displayed in the Figure 9. Note that the data tends to separate into three clusters which represent the fresh, once-burned, and twice-burned fuel sub-batches; each of which have much less spread than present in the 1813 individual data points used for the previous un-collapsed WLS regression.

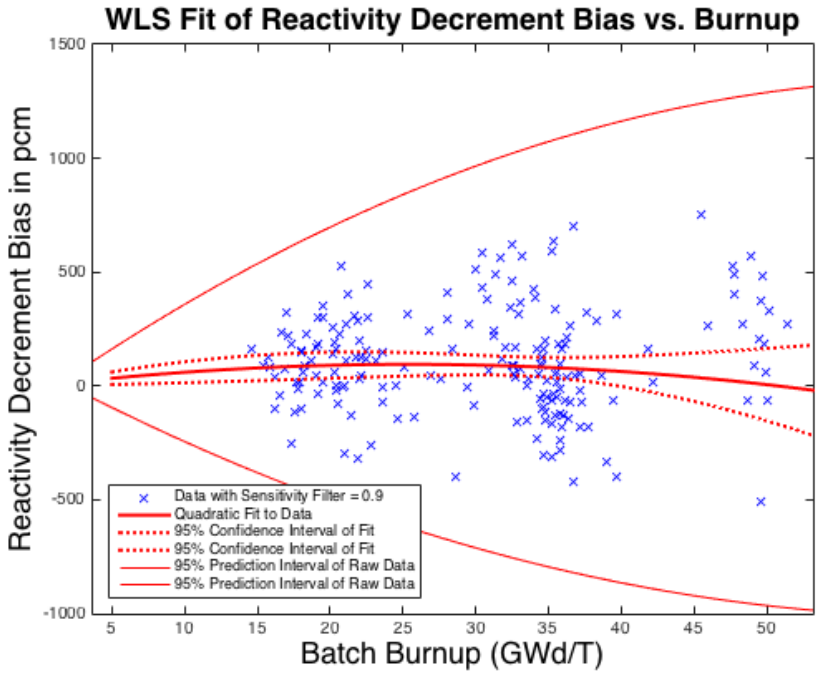

Figure 9 Reactivity Decrement Quadratic Regression For Cycle-collapsed Data

For Step 7, the residuals (differences between the data points and the regression fit) were used in a Shapiro-Wilk test to determine if the data "passes the normality test," as is required for confidence intervals to be correctly applied to the regression fits. As can be seen from the results in Figure 10, the residuals pass the Shapiro-Wilk normality test, as well as the Kolmogorov-Smirov/Lillefor test and D'Agostino normality tests.

Note that the maximum width of the 95% confidence interval in Figure 9 is 174 pcm at the high burnup end of the regression. The important point to recall here is that with the intra-cycle data points having been compressed to a single value, there are no correlation effects between successive flux map measurement points to be considered, and these regression confidence intervals can now be justifiably used - since the residuals correspond to the normal distribution needed for inferring the 95% confidence intervals for the regression fits.

For Step 8A, the data was divided into enrichment ranges above and below 4.35% enrichment, so that there are approximately 900 data points in both the high and low enrichment ranges. A quadratic regression was performed for each enrichment range as displayed in Figure 11 (high enrichment range)

and Figure 12 (low enrichment range). The maximum difference in the reactivity decrement bias vs. burnup is only 61 pcm at about 25 GWd/T burnup.

Normality Tests			
Variable #1 (Reactivity Decrement Bias Residuals)			
Sample size	**191**	***Mean***	**29.55241**
Standard Deviation	**238.40969**	***Median***	**0.**
Skewness	**0.26044**	***Kurtosis***	**2.92461**
Skewness (Fisher's)	**0.26251**	***Kurtosis (Fisher's)***	**-0.04532**
	Test Statistics	***p-level***	***Conclusion: (5%)***
Kolmogorov-Smirnov/Lilliefor Test	**0.05113**	**0.26167**	***No evidence against normality***
Shapiro-Wilk W	**0.99074**	0.25799	***Accept Normality***
D'Agostino Skewness	**1.50023**	**0.13356**	***Accept Normality***
D'Agostino Kurtosis	**0.01457**	**0.98837**	***Accept Normality***
D'Agostino Omnibus	**2.25089**	**0.32451**	***Accept Normality***

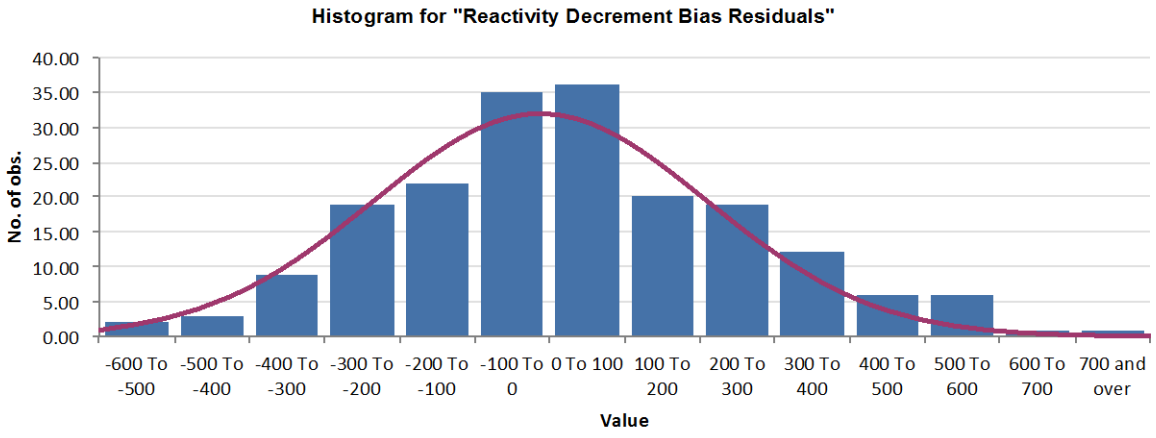

Figure 10 Normality Tests Of Cycle-collapsed WLS Regression Residuals of Figure 9 Data

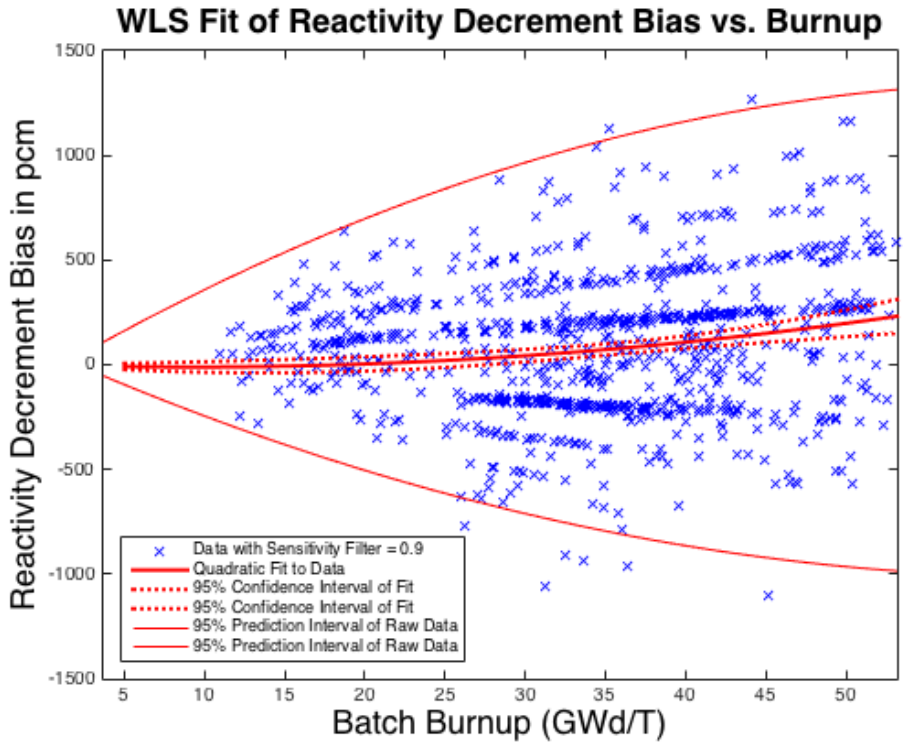

Figure 11 High Enrichment Sub-batch Reactivity Decrement Quadratic Regression

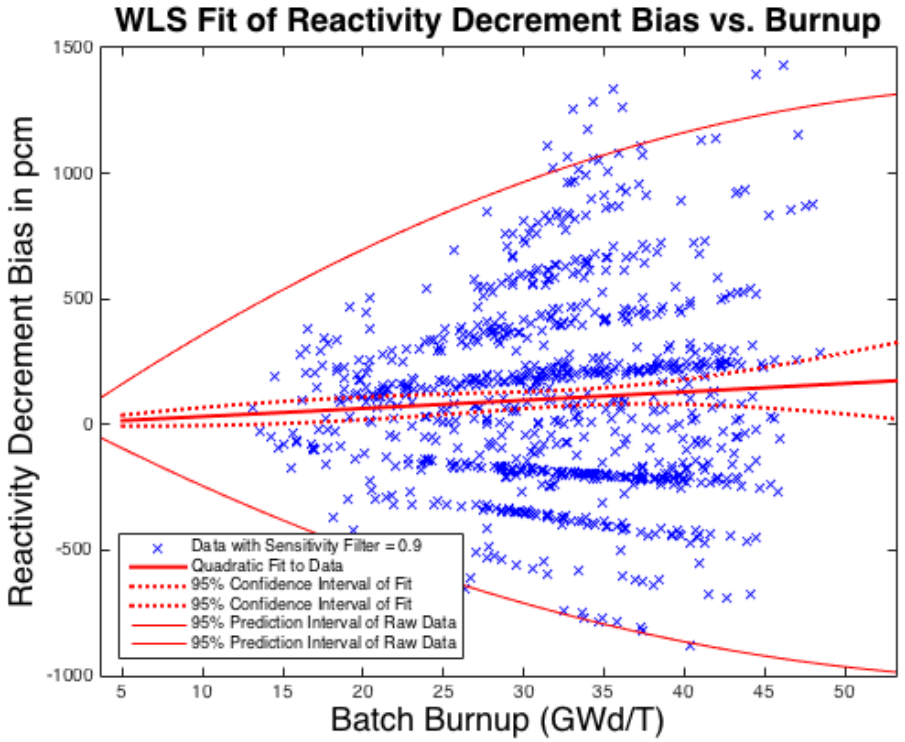

Figure 12 Low Enrichment Sub-batch Reactivity Decrement Quadratic Regression

For Step 8B, the absolute value of the differences (column 5) between the reactivity decrement biases of the high enrichment case (column 3) and low enrichment case (column 4) are added to the 95% confidence intervals (column 7) of the fully collapsed sub-batch/cycle regression fit (column 6), to obtain the "Augmented 95% Confidence Interval", as displayed in column 8 of Table 1.

Table 1 Summary of WLS Regression Results and Computation of the 95/95 Final Tolerance Limits

Reactivity Decrement Bias versus Burnup								
Burnup	No Correlation Bias	High Enrich	Low Enrich	Delta Enrich	Cycle Correlation Bias	95% C.I.	Augmented 95% C.I.	95% Tolerance Limit
5.0	4.7	-8.5	15.9	-24.4	33.8	27.5	51.9	56.5
10.0	12.5	-10.7	31.9	-42.6	60.1	46.0	88.6	96.5
15.0	23.4	-6.7	48.0	-54.7	79.1	55.8	110.5	120.3
20.0	37.3	3.7	64.2	-60.5	90.8	57.4	117.9	128.4
25.0	54.4	20.3	80.5	-60.2	95.1	51.9	112.1	122.0
30.0	74.6	43.2	96.9	-53.7	91.9	43.3	97.0	105.5
35.0	97.9	72.4	113.4	-41.0	81.5	43.5	84.5	92.0
40.0	124.3	107.9	130.0	-22.1	63.6	65.8	87.9	95.7
45.0	153.8	149.7	146.7	3.0	38.4	106.1	109.0	118.7
50.0	186.4	197.7	163.5	34.2	5.8	158.9	193.1	210.2

For Step 8C, the Augmented 95% confidence intervals are multiplied by the ratio of the two-sided 95/95 tolerance limit factor for to the 95% Student's t-value for 191 sub-batch/cycles data points, to obtain the 95/95 confidence limits – which are displayed in the last column of Table 1. Since there are 191 data points, this ratio is only 1.088, and differences between confidence intervals and tolerance limits is not very large given the large number of data points.

Note that the Student's t-value is used in constructing regression confidence intervals, and here we are making use of the fact that the underlying distribution of residual errors is Gaussian – as shown by the Shapiro Wilk test.

Conclusions

Statistical analysis has been used to arrive at new confidence limits for the measured HFP reactivity decrement biases of CASMO-5. One can be even more conservative and add the **maximum absolute delta** of the high to low enrichment bias difference (61 pcm) to the **maximum width of the collapsed WLS confidence interval** (170 pcm; within the largest burnup of any sub-batch, 53.2 GWd/T) and apply the **tolerance factor ratio** (1.088), to obtain a **single value for the regression upper confidence limit – which is 252 pcm**.

This confidence limit is nearly identical to the 250 pcm 95% uncertainty estimated in Table 7-1 of the original EPRI/Studsvik report [1], by completely non-statistical methods (e.g., measuring the uncertainty introduced from a known magnitude defect in the CASMO cross section library).

Table 7-1
Measured CASMO-4 Reactivity Decrement Bias (change needed to match measurement)

Burnup (GWd/T)	10.0	20.0	30.0	40.0	50.0	60.0
CASMO-4 Bias (pcm)	81	140	178	196	192	167
CASMO-5 Bias (pcm)	19	46	81	125	177	238
Uncertainty (pcm)	250	250	250	250	250	250

Note also that the CASMO-5 reactivity decrement bias in Table 7-1 is within approximately 10 pcm of the column 2 data from the WLS regression fits displayed in Table 1 (corresponding to Figure 6).

It is also important to recall that the HFP 95/95 confidence limit will ultimately be combined with the TSUNAMI HFP-to-Cold 95% uncertainty to arrive at a final measured cold reactivity decrement bias and uncertainty, as displayed in Table 10-1 of the EPRI/Studsvik report [1].

Table 10-1
CASMO Measured Cold Reactivity Decrement Bias and 2σ Uncertainty (delta-k in pcm)

Burnup (GWd/T)	10.0	20.0	30.0	40.0	50.0	60.0
CASMO-4 Bias (pcm)	81	140	178	196	192	167
CASMO-5 Bias (pcm)	19	46	81	125	177	238
95% Uncertainty (pcm)	521	576	571	560	544	534

Since the HFP 95/95 confidence limit is small compared to the hot-to-cold uncertainty, small changes in HFP confidence limits will contribute very little to the final 95% uncertainty. As such, the conclusions of that report remain valid, **and there is no need to update the EPRI Reactivity Decrement Benchmarks** [1] derived from that work.

References

1. K. S. Smith et al., “Benchmarks for Quantifying Fuel Reactivity Depletion Uncertainty,” Technical Report 1022909, EPRI, Palo Alto, CA, (2011).

2. G.A. Gunow, “LWR Fuel Reactivity Depletion Verification Using 2D Full Core MOC and Flux Map Data,” M.S. Thesis, MIT, https://dspace.mit.edu/handle/1721.1/97963, (2014).

3. E. Sykora, “Testing the EPRI Reactivity Depletion Decrement Uncertainty Methods,” M.S. Thesis, MIT, pending MIT, dspace.mit.edu/handle assignment, (2015).